Study of Process Characteristics of Friction Stir Lap Welded AZ31B Alloy and AISI304

Kumar Sawrav[a]*, Abhishek Gupta[a]
Department of Mechanical Engineering, Indian Institute of Technology Kharagpur, Kharagpur, West Bengal, India, Pin 721 302
*Corresponding Author. E-mail address: kumarsawrav@gmail.com

ABSTRACT

The weight reduction by improving the material properties is always a challenge which has been achieved by joining of lightweight materials. Some steel components can be replaced by lightweight materials like magnesium alloy. Magnesium has low density and high strength to weight ratio. The main difficulty in joining of magnesium and steel with traditional fusion welding techniques is their melting point difference of 900°C and low solubility. To solve the problem of joining of dissimilar metals, the solid-state welding such as Friction stir welding has potential to join these materials. In this work, the process characteristics were studied for Friction Stir Welding of Magnesium alloy (AZ31B) and Stainless steel (AISI304) in lap configuration. Various sets of experiment were carried to study the effect of process parameters i.e., plunge depth and tilt angle on force, temperature, mechanical strength and microstructure, grain structure. Tensile test and micro-hardness indentation have been carried out to evaluate the mechanical properties. Later the joint interface has been characterized with the help of SEM, XRD and optical microscopy. Results suggested deeper penetration of tool has detrimental effect on the mechanical strength due to excess hooking effect. Also grains refinement has been found in the welded region. XRD results indicated formation of inter-metallic compound at the joint interface.

Keywords: Dissimilar metals, Friction Stir Welding (FSW), magnesium alloy, lap configuration.

Tob Regul Sci. ™ 2021;7(6-2): 78-93
DOI: doi.org/10.18001/TRS.7.6.2.9

1. Introduction

Friction stir welding (FSW) is a solid-state joining technique invented at The Welding Institute (TWI) of the United Kingdom in 1991[1]. The principle of FSW is based on thermo- mechanical effect where a non-consumable rotating tool with a specially designed pin and shoulder is inserted into the abutting edges of sheets or plates to be joined and subsequently traversed along the joint line (Fig. 1). FSW tool has the following purposes:

a) Heating of the work material due to the friction between shoulder and workpiece surface causing plastic deformation of work material.

b) Mixing of the material whose yield stress value decreases due to the increase in temperature of the workpiece or in other words material get plasticized at a higher temperature.
c) Contain the hot plasticized metal beneath the shoulder.

The shoulder and pin, while rotating, meets the plate surface. The relative motion and the friction between the FSW tool and the plate results in frictional heat and mechanical stirring. The frictional heat raises the temperature of the plate around the tool and bring it in softens state by reducing the yield strength. As the material gets softer, it easily gets stirred. The traverse movement of the tool causes the flow of material from the front of tools shoulder to the trailing edge where it gets consolidated under the effect of shoulder. Tilting of tool towards the trailing edge provides an additional forging pressure which stops the flash formation and avoids weld defects. Since the whole welding process takes place in the solid state, so the defect such as porosity, blow holes, etc. were absent.

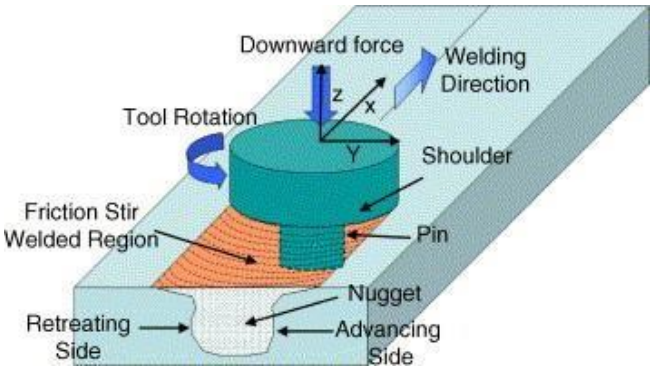

Fig. 1: Schematic of FSW [1]

1.1 Dissimilar material welding

Today energy saving and controlling degradation of the environment because of the emission of harmful greenhouse gases are important problems that need to be tackled immediately. Reducing the weight of the vehicle would be one of the finest and economic counter- measures. By reducing vehicle weight by 10% results in 8-10% of saving in fuel economy and reduces the greenhouse gas emission. This weight reduction can be achieved by

i. Replacing the high-density steel by low-density alloys like magnesium or aluminum alloy
ii. By using advanced lightweight, high strength steel.

Magnesium makes a better choice because it has 1.8 g/cm^3 of density which has five times lower than steel, higher specific strength and specific stiffness as compared to steel. Also, they are abundantly available, and they are recyclable.

2. Literature review

Joining of Mg and steel has been carried out by laser welding, but it has difficulty in welding due high melting temperature difference and low solubility between steel and magnesium alloy. Due to the high melting temperature difference, there was the formation of porosity and welding cracks in the weld.

Liu and Zhao tried using TIG and laser-TIG hybrid welding respectively for joining of AZ31B and AISI304. It was found that magnesium alloy burned, and oxide formation occurs [2]. Y. Abe et al. studied the dissimilar metal butt joining of magnesium alloy and mild steel. In this paper, AZ31B-O and AISI 400 were butts welded using FSW. Fracture occurred at the weld interface for low rotating speed, strength was less due to insufficient plasticization of the magnesium. At very high welding speed ignition occurs in the magnesium which reduces the strength [3]. Y.C. Chen and K. Nakata studied the joining of magnesium alloy and zinc coated low carbon steel in the lap configuration using friction stir welding. Maximum failure load of welded was found to be 65% of the zinc coated base metal. Increasing the welding speed decrease the failure load as it decreases the heat input which reduces the reaction between Mg alloy and zinc coated steel. the weld [4]. Y.C. Chen and K. Nakata studied the effect of tool geometry on microstructure, and mechanical properties of friction stir lap welded magnesium alloy and steel. [5]. Y. C. Chen and K. Nakata studied Effects of surface states of steel on microstructure and mechanical properties of lap joints of magnesium alloy and steel by friction stir welding [6]. Jana et al. have studied the effect of dynamic loads on microstructure evolution and fracture loading of lap weld of AZ31 Magnesium Alloy and steel (High strength low alloy and mild steel). The tool used for the process was made from H13 [7]. Schneider et al. have studied the effect of welding speed on mechanical properties and temperature near the weld. The AZ31 magnesium alloy and ultra-low carbon steel were chosen in lap configuration for experimentation. It was concluded that the fracture strength of the weld goes on increasing with increasing the welding speed [8]. Yanni et al. have studied the effect of welding speed and tool design on mechanical properties and microstructure evolution of lap joint of AZ31B magnesium alloy and SUS302 steel. The nail effect by long flashes and zipper effect by saw tooth are responsible for enhancing joining strength at high travel speed [9].

Kasai et al. have investigated the effect rotational speed on the joint strength and evolution of the inter-metallic (Fe-Al) compounds at the butt weld interface of pure magnesium and it is AZ31 AZ61 alloys [10].

While going through the literature survey following gaps were observed and the presented work here has motivation & novelty for the overall analysis.

- Effect of overlapping length and position of magnesium sheet can be investigated.
- It was observed that the effect of various tool rotational speeds on force, temperature, mechanical and metallurgical properties was not studied yet on lap configuration of magnesium alloy and steel.
- Effect of tool tilt angle and plunge depth on mechanical properties of joint in lap andbutt configuration.
- Investigation of Zn layer thickness on corrosion behavior.
- Different tool geometries and their effect on mechanical properties can be investigated.

The aim of the current work was to study the effect of tilt angle and plunge depth on the axial force, temperature and mechanical properties in friction stir lap welding of AZ31B and AISI 304. The following aspect were investigated for friction stir lap welding of magnesium and steel sheets:

- Effect of tilt angle and plunge depth on force generation during welding
- Effect of tilt angle and plunge depth on temperature in weld zone during welding
- Effect of tilt angle and plunge depth on shear, tensile load, and elongation

- Analysis of the hardness along the joint and perpendicular to joint
- Fractography study of welded specimen to find the mode of fracture
- Interface study to know the different types of bonding present at the interface whichstrengthen the joint.

3. Experimental details

In this study Magnesium alloy (AZ31B) and Stainless steel (AISI304) were used as base materials. The chemical composition was determined by Optical microscopy (OES) and are given below in Tables 1 and 2. The dimension of the workpiece was 100 mm×80 mm×1.5 mm for AZ31B and 100 mm×80 mm×1 mm for AISI304. Physical properties of the materials are listed in Table 3. Magnesium sheet was kept on the steel sheet, and the overlapping length was 35 mm. Fig. 2 shows the schematic representation of FSLW of AZ31B and AISI 304 sheets. Magnesium alloy was kept on advancing side and steel was kept on retreating side.

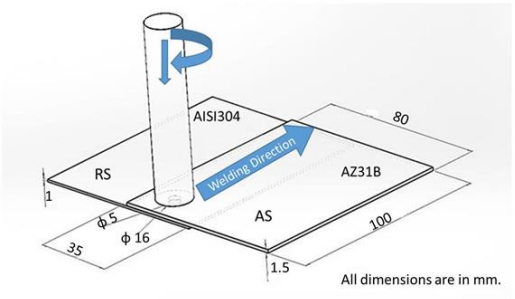

Fig. 2: Schematic representation of FSLW of AZ31B and AISI304

Table 1: Chemical Composition of AZ31B Magnesium alloy

Elements	Al	Zn	Mn	Si	Cu	Fe	Ni	Mg
Composition	2.97	0.82	0.44	0.033	0.0076	0.0029	0.00076	Bal

Table 2: Chemical Composition of AISI 304 steel

Elements	C	Cr	Fe	Mn	Ni	P	S	Si
Composition	0.073	19	68.64	1.6	9	0.036	0.03	0.7

Table 3: Physical properties of AZ31B Magnesium alloy and AISI 304 Steel

Material	Density (g/cm^3)	Tensile Strength (MPa)	Hardness (HV)	Melting point (°C)
AZ31B	1.77	236	84	660
AISI304	8	600	281	1673

For the FSW of the magnesium and steel, the tool should withstand high temperature and should have high melting point and strength. So, tool made of tungsten carbide (C2-WC) was used as it had desired

properties. The dimension of the tools shoulder diameter 16 mm, pins diameter was 5 mm and pin height 1.6 mm (Fig.3).

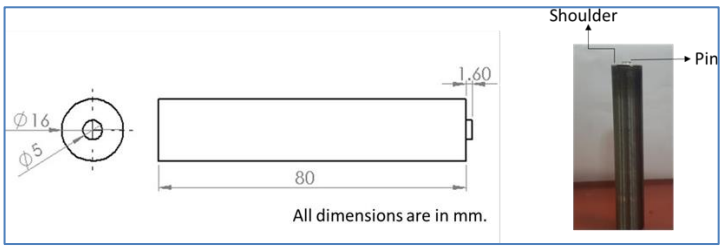

Fig.3: FSW Tool

Sheets of the AZ31B and AISI 304 were lap welded using 3-axes vertical CNC controlled friction stir welding machine (Fig.4). The experimental setup is shown in Fig.5. Total nine experiments were carried out using different process parameters. Process parameters sets are given in Table 4. The experiments were performed by varying plunge depth and tilt angle keeping constant the rotational speed at 900 rpm and welding speed 300 mm/min. The temperature generated during welding was obtained by using K-type Thermocouples, and data acquisition card was used to get data with the help of LabVIEW software. Two thermocouples were embedded 3 mm away from the centerline, at the bottom of the magnesium sheets and towards the steel side at the starting point and 40 mm from the start point of the welding (Fig. 6). Force was measured by the inbuilt strain gauge type dynamometer of 3 axes CNC Friction Stir Welding machine. Connection for temperature measurement was shown in Fig. 7.

Fig.4: 3 axes CNC FSW machine

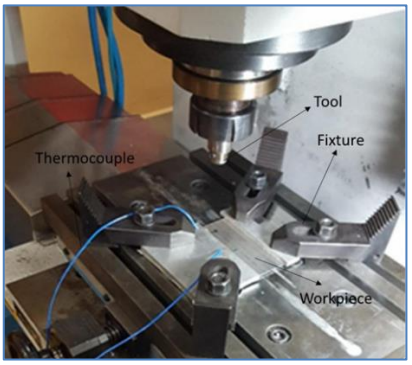

Fig.5: Experimental Setup

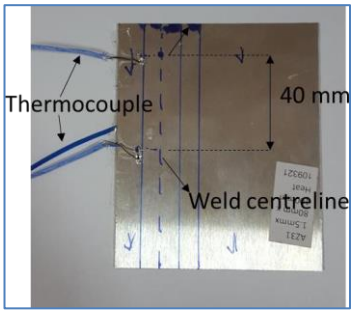

Fig.6: Thermocouple embedded into the Mg sheet

Fig.7: Connection for temperature measurement

Block diagram for temperature measurement

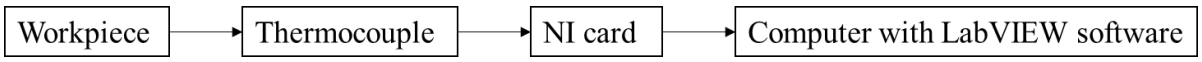

Table 4: Process parameters for experiments

Exp No.	Rotation speed	Welding speed	Plunge depth	Tilt angle
1	900 rpm	300 mm/min	0.1mm	0^0
2			0.2mm	0^0
3			0.3mm	0^0
4			0.1mm	1^0
5			0.2mm	1^0
6			0.3mm	1^0
7			0.1mm	2^0
8			0.2mm	2^0
9			0.3mm	2^0

The shear tensile test was carried out in the universal tensile test machine (INSTRON 3365) with a constant crosshead velocity of 1 mm/min. For lap shear testing the specimen was cut normal to the weld line by the Wire EDM machine (Elektra, Maxicut 523). The dimensions of tensile -shear specimen was 35 mm gauge length, 10 mm gauge width and 1.5 mm gauge thickness (Fig 8)

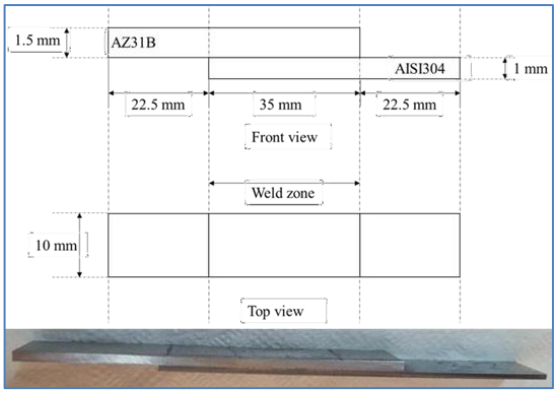

Fig.8: Tensile shear test specimen

Vickers hardness test has been carried out measure the microhardness. Vickers microhardness test was done using microhardness testing machine (UHL, VMHT) at a load of 100 g and a dwell time of 15s.

Optical microscopic study (OM) has been done by using an inverted metallurgical microscope (Leica, DMILM), to measure grain size using the image of the microstructure and to check the different types of

bonding between Mg and steel at the interface. For optical microscopy samples were cold mounted and were prepared by polishing using abrasive papers of grade 220,600,1000,2000,4000 and final polishing was done by the diamond abrasive on the variable speed grinder polishing machine (Buehler, Ecomet 3000). For grain structure chemical etching of the polished sample was done using etchant A qua regia (1:3 solution of conc. HNO_3 and HCl), and for magnesium alloy, a solution of 4.2 g picric acid, 10 ml acetic acid, 66 ml ethanol and 10 ml water was used. The joints were examined using scanning electron microscope (SEM) with X-ray energy dispersive spectroscopy (EDS) for bonding mechanism and to find the formation of intermetallic compound (IMC) at the interface. Fractography was done in the SEM to study the type of fracture.

4. Results and discussion

4.1 Force measurement

Variation of axial force (Fz) with respect to time at rotation speed of 900 rpm, welding speed of 300 mm/min, plunge depth of 0.1 mm, and tilt angle 0° has been shown in Fig 9, which shows the evolution of plunge force with time. It can be seen from the graph that as the tool pin meets the workpiece, force starts to rise further, once the pin has completely plunged, the material comes to a plastic stage, the force becoming nearly constant as it can be seen from the graph. The sudden rise in the force was due to the contact of the shoulder with the workpiece. As soon as the plunging stage was completed, the travel of the tool begins, and the graph becomes again constant.

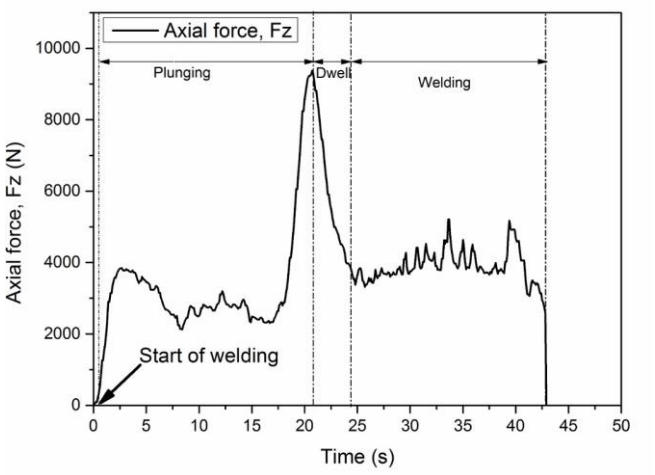

Fig. 9: Variation of axial force with time

4.1.1 Effect of tilt angle on average axial force and torque

The average value of axial force (Fzavg) has been calculated from plunge into the end of the welding operation. The effect of the tilt angle on the Fzavg has been show in the Fig 10. It could be seen that increasing the tilt angle increases the axial force. The results obtained in the figure was taken at a constant rotational speed of 900 rpm and welding speed of 300 mm/min. This increase in force can be attributed to an effective increase in plunge depth (plunging of the shoulder) at the trailing edge of the weld. The

increase in plunge depth
resulted in increased forging action on the weld and thereby increasing the force. Effect of tiltangle on the torque has found to be having same as the effect on the force (Fig 11).

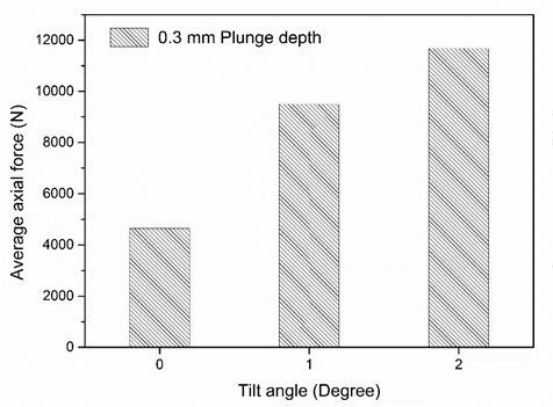

Fig. 10: Effect of tilt angle on average axial force

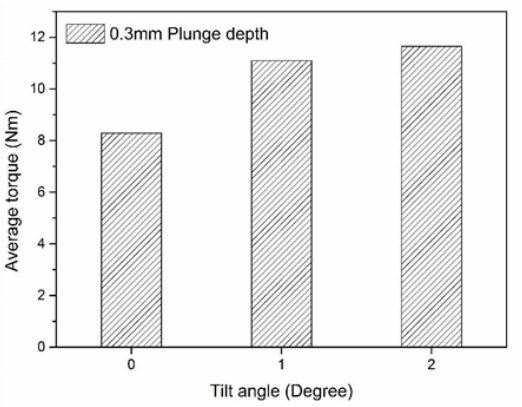

Fig. 11: Effect of tilt angle on average torque

4.2 Effect of plunge depth on average axial force and torque

The effect of the plunge depth on the Fzavg has been show in the Fig.12. The results obtained in the figure was taken at a constant rotational speed of 900 rpm and welding speed of 300 mm/min. It could be seen that increasing the plunge depth increases the axial force because shoulder goes deeper into the workpiece, and it moves greater volume of material. Effect of plunge depth on the torque has found to be having same as the effect on the force (Fig13).

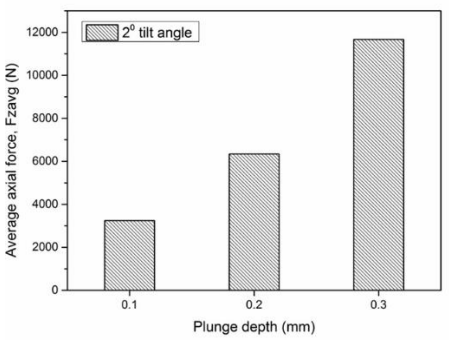

Fig. 12: Effect of plunge depth on the average axial force

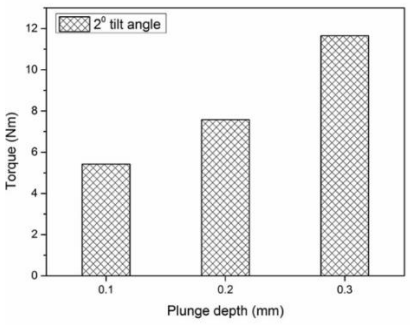

Fig. 13: Effect of plunge depth on the Torque

4.3 Temperature measurement

The temperature reading was taken along retreating side. Two thermocouples (Tc0 and Tc1) were fixed one at the starting point of the weld and other at 40 mm from the starting point (Fig 14). When the tool plunging starts, the temperature in the first thermocouple rises rapidly and reaches a maximum of 294°C but as welding starts temperature decreases in first thermocouple and in second thermocouple it starts to increase until it reaches a maximum value of 320°C when tool reaches that point. When the tool moves away from the thermocouple temperature starts to decrease rapidly. This shows that rate of cooling of the material was more than that of the heat conduction rate.

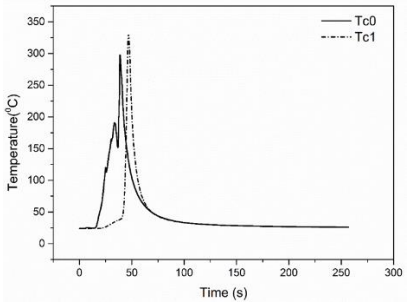

Fig. 14: Variation of temperature with time

4.4 Effect of tilt angle on the peak temperature

The effect of tilt angle on the peak temperature is shown in Fig.15, in which the process parameter set were rotational speed of 900 rpm, welding speed of 300 mm/min and plunge depth of 0.3 mm. Increasing tool tilt angle increases axial forces and decreases plastic deformation. This leads to high heat generation in the workpiece which increases the peak temperature.

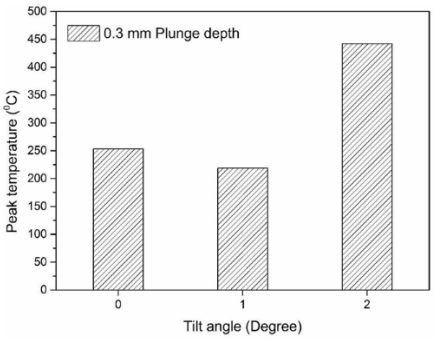

Fig. 15: Effect of tilt angle on the peak temperature

4.5 Effect of tilt angle and plunge depth on the tensile load

Fig.16 shows the effect of tilt angle and plunge depth on the tensile load. The maximum value of the tensile load was 2110 N at a rotational speed of 900 rpm, a welding speed of 300 mm/min, plunge depth 0.2 mm and tilt angle 1°. The maximum welding efficiency of 58.2% was obtained. As from the Fig.16 for 1° tilt angle tensile load decreases with increasing the plunge depth due to increase in length of the hook. So, there will be stress concentration in the specimen which decrease the strength. For 0° and 2° tilt angle maximum tensile load occur at

0.2 mm plunge depth. It was found that when plunging depth increases from 0.1 mm to 0.2 mm the tensile load increases and further increase in plunging depth to 0.3 mm the tensile load decreases. At 0.1mm plunging depth, the tool shoulder generates less amount of heat compared to 0.2mm plunging depth which leads to poor joint strength. When plunging depth increases to 0.3mm, the heat generation was more but local thinning occurs at the shoulder workpiece interface area which leads to poor weld strength. So, among all the three level of plunging depth, 0.2mm plunging depth gives better tensile load compared to 0.1mm and 0.3mm plunging depth. Fig.17 shows the plot of tensile load with extension for AISI304, AZ31B and welded sample with parameters of 900 rpm rotational speed, 300 mm/min welding speed, 0.2 mm plunge

depth and 2° tilt angle. It can be seen from the figure that strength of AZ31B was nearly half of the AISI304. The strength of welded sample was nearly 60% of the base AZ31B.

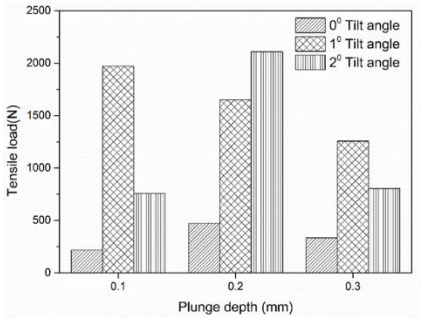

Fig. 16: Effect of tilt angle and plunge depth on the tensile load with welded samples

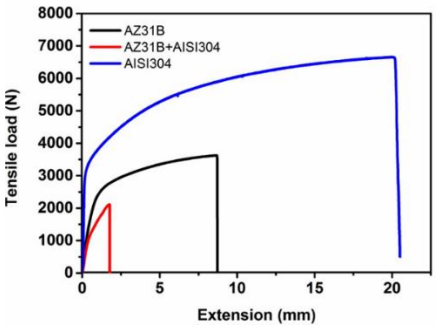

Fig. 17: Tensile load with extension for base materials

4.6 Fractography

To investigate the mode of fracture for welded joint SEM images of fracture surfaces of some samples have been taken. Fig. 18,19,20,21,22 shows the SEM images of fractured surfaces for different combination of plunge depth and tilt angle. At PD of 0.1 mm and tilt angle of 0° a river line pattern was observed on the fractured surface which indicate brittle failure of the sample. Elongation was only 0.71%. At PD of 0.3 mm and tilt angle of 0° a river line pattern was observed on the fractured surface which indicate brittle failure of the sample. Elongation was only 0.85%. At PD of 0.2 mm and tilt angle of 1° a dimple pattern with some steel particle trapped were observed on the fractured surface which indicate ductile failure of the sample. Elongation in this case was 2.34%. At PD of 0.2 mm and tilt angle of 2° a dimple pattern and river line pattern were observed on the fractured surface which indicate brittle-ductile failure of the sample and in this case, elongation was 5.2%. At 0.3 mm plunge depth increasing tilt angle shift ductile mode of failure to brittle-ductile mode of failure.

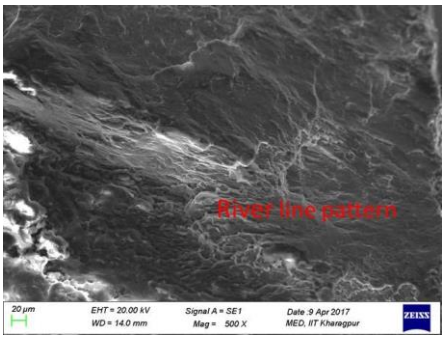

Fig. 18: SEM image of the fractured sample for PD of 0.1 mm and θ of 0°

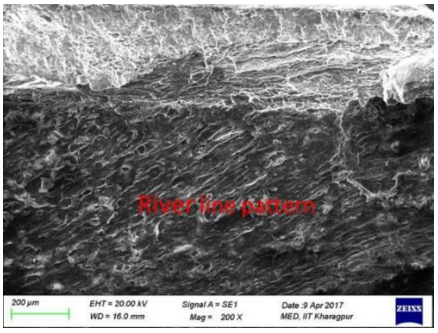

Fig. 19: SEM image of the fractured sample for PD 0.3 mm and θ 0°

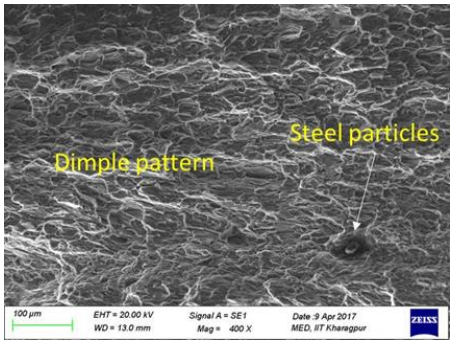

Fig. 20: SEM image of the fractured sample for PD 0.2 mm and θ 1°

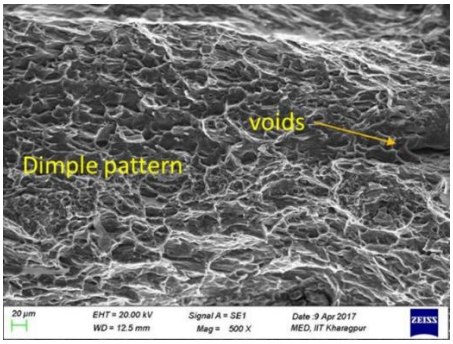

Fig. 21: SEM image of the fractured sample for PD 0.3 mm and θ 1°

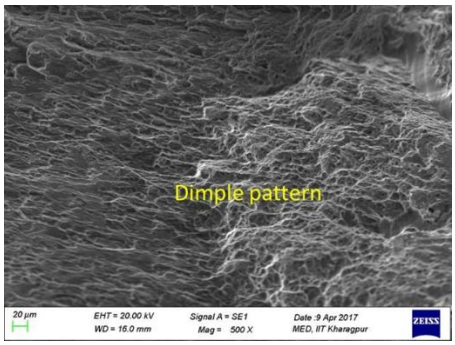

Fig .22: SEM image of the fractured sample for PD 0.2 mm and θ 2°

4.7 Interface characterization

Fig 23, 24, 25 shows the SEM image for the welding parameter of rotational speed 900 rpm, welding speed 300 mm/min and tilt angle 1°. As from the figures we can see increasing the plunge depth increases the hook length formed in the joints. Increased hook length results in the stress concentration in the weld which decreases the tensile load. There were voids present in the near the hook which also results in the decreased strength of the weld. Failure of the joints occur near the hook.

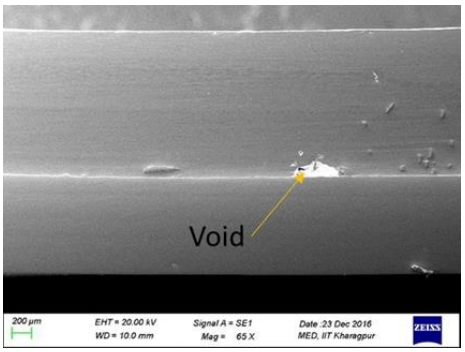

Fig. 23: SEM image for 0.1 mm plunge depth

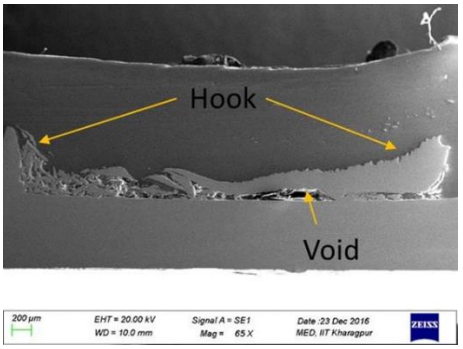

Fig. 24: SEM image for 0.2 plunge depth

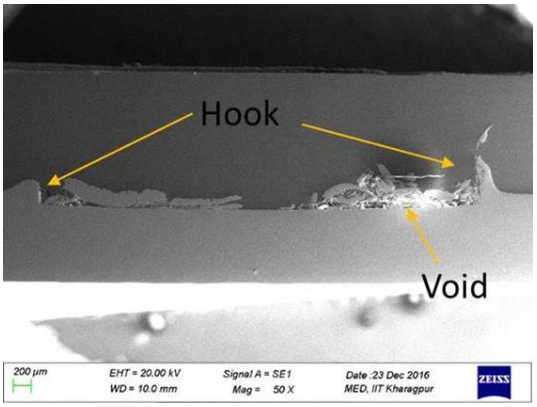

Fig. 25: SEM image for 0.3 mm plunge depth

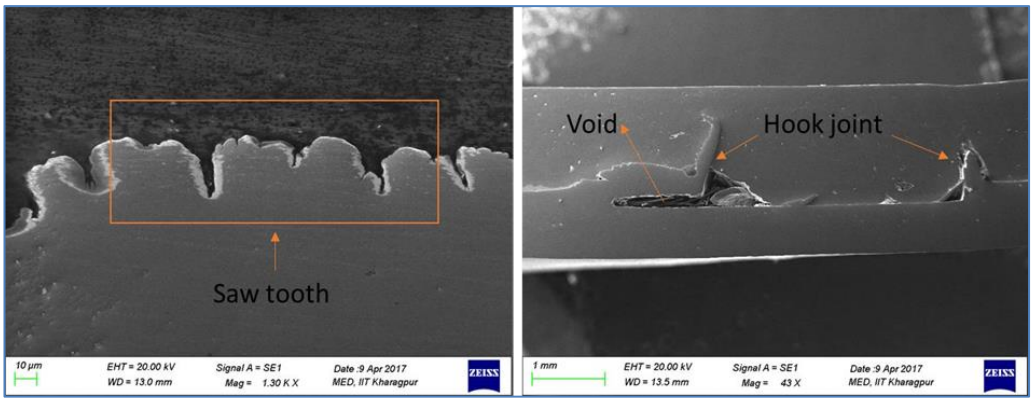

Fig. 26: Different bonding mechanisms at 0.1 mm PD and 0° θ

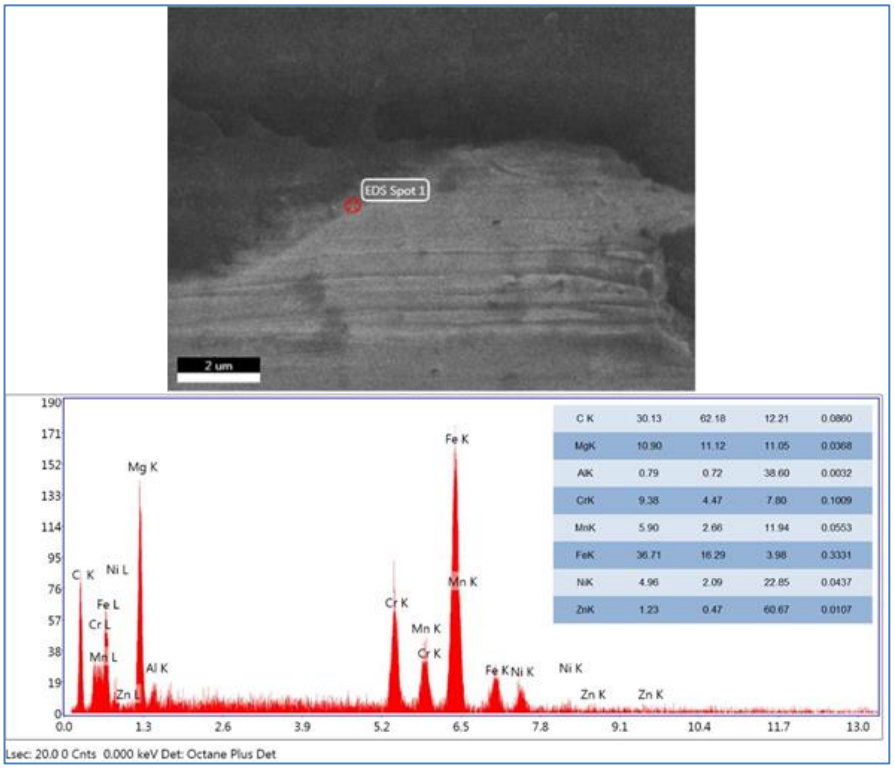

Fig. 27: SEM image and point EDS analysis at the joint interface

In friction stir lap welding of magnesium and steel different types of mechanical and chemical bonding were present. These different types of bonding at the interface make the joint between magnesium and steel stronger. Fig.26 shows the different bonding mechanism at 0.1 mm PD and 0° of tilt angle (θ). Two types of mechanical bonding visible in the above image were hook joints and saw tooth. Apart from mechanical bonding intermetallic compound were also formed. Hook joint (Macro interlocking) strengthen the weld by nail effect and saw tooth interface by zipper effect in friction stir lap welding of Magnesium and steel. Some defects were present as voids beside hook joint, at the middle of the nugget zone near interface. Defects at the weld region did not affect the joint strength as most of the cases fracture took place at heat affected zone. Fig.27 shows the SEM image and point EDS at the joint interface. Point EDS analysis shows the formation of intermetallic compound (IMC). Possible IMC of Al/Mg or Fe/Zn were formed. To find the phase of IMC further XRD test were done.

4.8 Microstructural characterization

Fracture occurs in the stir zone. Fig.28 shows the microstructure of the SZ and HAZ of the welded sample. Grain size in SZ was 9.11 μm and in HAZ was 8.65 μm. Grain size was more on the SZ than HAZ. Large grain decreases ductility of material, so fracture occur at SZ.

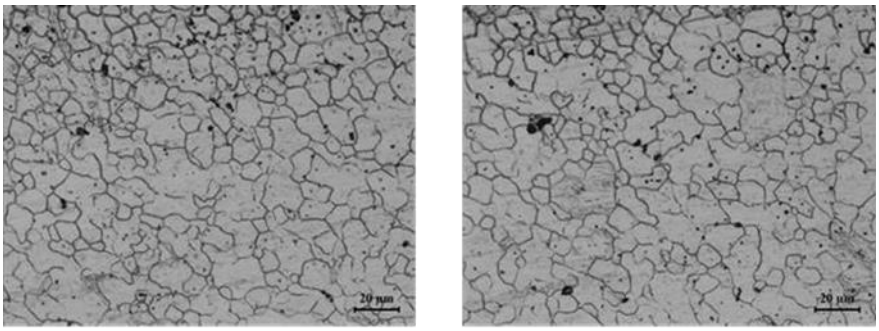

Fig. 28: Variation of grain size (a) SZ (b) HAZ

4.9 Hardness measurement

Vickers hardness measurement was done to find the micro hardness of the welded sample for a rotation speed of 900 rpm, a welding speed 300 mm/min, plunge depth of 0.2 mm and a 1° tilt angle. Variation of micro hardness with distance from top of Mg sheets has been shown in Fig. 29. In Fig.29 as we move from top to bottom of the micro hardness increases and reaches the maximum value at the interface as we go away from the interface hardness value decreases. Same trend in stir zone, retreating side and advancing side follows for the hardness.

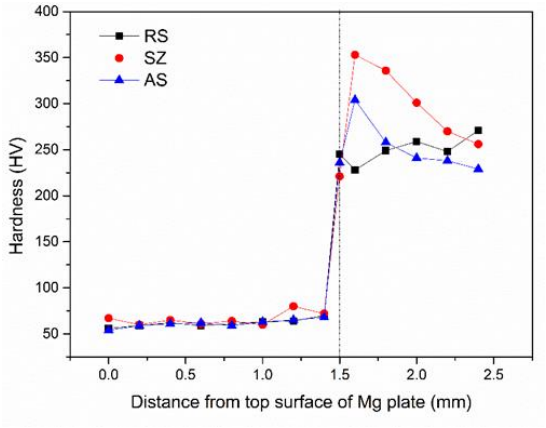

Fig. 29: Variation of micro hardness from the top surface of Mg plate

Variation of hardness from retreating side to advancing side at 0.5 mm above interface towards Mg has been shown in Fig. 30. It was found that as plunging depth increases from 0.1 mm to 0.2 mm the hardness value also increases due to grain refinement as heat generation rate was more. Increasing more plunge depth decreases hardness as more heat generation takes place which increases grain growth. From the figure the hardness at the stir zone was high as compared to the RS and AS. High value of hardness at the stir zone was due finer grain caused by dynamic recrystallization.

Hardness at the hook formed in the interface were measured. Values of hardness found were 502 HV, 440 HV, and 417 HV which were higher than the hardness of steel at the stir zone. This can be possible because of formation of intermetallic compound.

The XRD test of the sample has been carried out over the welded surface. Several phases were found. An IMC of $Al_{12}Mg_{17}$ can be seen on the XRD pattern. In addition to that, IMC of $FeZn_{15}$ can be seen. The presence of zinc in the AZ31B alloy resultsin the formation of iron-zinc compound (Fig. 31).

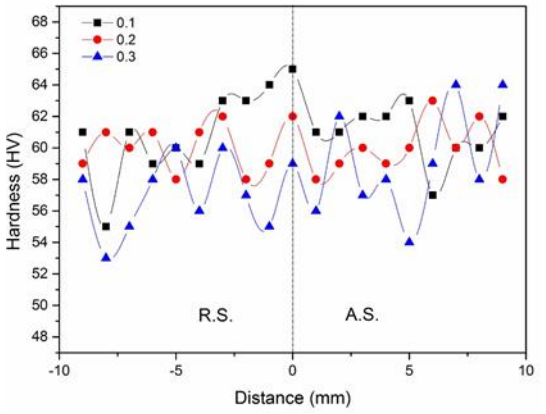

Fig. 30: Variation of micro hardness with different plunge depth

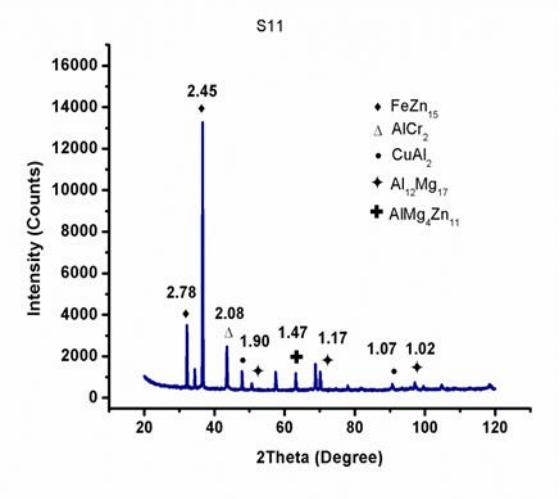

Fig. 31: XRD pattern on the welded surface at 0.1 mm PD and 0° θ

5. Conclusions

Friction stir lap welding has been successfully carried out to join AZ31B and AISI304.Thefollowing conclusions were made from the experimental study.

1. Maximum tensile load of 2110 N was obtained for rotational speed of 900 rpm,welding speed of 300 mm/min, plunge depth of 0.2 mm and tilt angle of 1°.
2. The welding efficiency of 58.2% was obtained.
3. Increasing the tilt angle increases the average axial force and average torque.
4. Increasing the plunge depth increases the axial force because shoulder goes deeper into the workpiece, and it moves greater volume of material
5. During plunging two peak forces were generated. First peak force at the start of the plunging when pin moves inside the surface of Mg plate and other was when pin touches the steel plate.
6. Peak temperature increases with increase in tilt angle.
7. Maximum temperature during welding was found to be 320°C which lower than themelting temperatures of the magnesium alloy. So, joining was pure solid state joining.
8. Tensile load decreases with increase in plunge depth for 1° tilt angle due to increase inthe length of the hook.
9. Mode of failure was ductile brittle.
10. For 0° and 2° tilt angle tensile load first increases by increasing plunge depth due toproper heat generation then it decreases due to formation of large hook joint.
11. Bonding mechanism was due to Hook formation, saw tooth, IMC formation at theinterface.
12. It was found hardness first increase with increase in plunge depth then decreases withmore plunge depth.
13. The maximum micro-hardness was observed at the weld nugget due to high thermalcycle, plastic deformation, and dynamic recrystallization.
14. Hardness shows the same pattern along thickness at weld nugget on retreating side,middle and advancing side.
15. IMC of $Al_{12}Mg_{17}$ and $FeZn_{15}$ were formed at the weld interface.

References

[1] R. S. Mishra and M. W. Mahoney, "Friction Stir Welding and Processing," *ASM Int.*, p. 368, 2007.

[2] Z. X. Yao, D. P. Jiang, C. Pan, and X. M. Wang, "Analysis about the Jointing Status for Dissimilar Metals of Steel with Magnesium," *Appl. Mech. Mater.*, vol. 233, pp. 374–379, 2012.

[3] Y. Abe, T. Watanabe, H. Tanabe, and K. Kagiya, "Dissimilar Metal Joining of Magnesium Alloy to Steel by FSW," *Adv. Mater. Res.*, vol. 15–17, pp. 393–397, 2007.

[4] Y. C. Chen and K. Nakata, "Friction Stir Lap Welding of Magnesium Alloy and Zinc- Coated Steel," *Mater. Trans.*, vol. 50, no. 11, pp. 2598–2603, 2009.

[5] Y. C. Chen and K. Nakata, "Effect of tool geometry on microstructure and mechanical properties of friction stir lap welded magnesium alloy and steel," *Mater. Des.*, vol. 30, no. 9, pp. 3913–3919, 2009.

[6] Y. C. Chen and K. Nakata, "Effect of the Surface State of Steel on the Microstructure and Mechanical Properties of Dissimilar Metal Lap Joints of Aluminum and Steel by Friction Stir Welding," *Metall. Mater. Trans. A*, vol. 39, no. 8, pp. 1985–1992, Aug. 2008.

[7] S. Jana, Y. Hovanski, and G. J. Grant, "Friction stir lap welding of magnesium alloy to steel: A preliminary investigation," *Metall. Mater. Trans. A Phys. Metall. Mater. Sci.*, vol. 41, no. 12, pp. 3173–3182, 2010.

[8] C. Schneider, T. Weinberger, J. Inoue, T. Koseki, and N. Enzinger, "Characterization of interface of steel/magnesium FSW," *Sci. Technol. Weld. Join.*, vol. 16, no. 1, pp. 100–107, 2011.

[9] Z. X. Yao, D. P. Jiang, C. Pan, and X. M. Wang, "Analysis about the Jointing Status for Dissimilar Metals of Steel with Magnesium," *Appl. Mech. Mater.*, vol. 233, pp. 374–379, 2012.is

[10] H. Kasai, Y. Morisada, and H. Fujii, "Dissimilar FSW of immiscible materials: Steel/magnesium," *Mater. Sci. Eng. A*, vol. 624, pp. 250–255, 2015.